

Article

Tensile Mechanical and Stress-Strain Behavior of Recycling Polypropylene Fiber Recycled Coarse Aggregate Concrete

Jianchao Wang ¹, Jiahe Liang ², Yucheng Li ^{2,*} and Wei Hou ³

¹ School of Science, Shenyang Jianzhu University, Shenyang 110168, China; wangjianchaook@sjzu.edu.cn

² School of Civil Engineering, Shenyang Jianzhu University, Shenyang 110168, China; liangjiahe_2021@163.com

³ School of Marxism, Shenyang Jianzhu University, Shenyang 110168, China; houwei@sjzu.edu.cn

* Correspondence: yucheng_li1@163.com

Abstract: To effectively recycle waste petroleum products and construction waste, recycling polypropylene fiber (RPF) and recycled aggregate can be mixed into concrete to make RPF recycled coarse aggregate (RCA) concrete. In this study, the RPF recycled from a polypropylene (PP) packaging belt was used as the test material and manually cut into the shape required for the experiment. The effects of RCA and RPF on the tensile mechanical behavior of concrete are researched. The failure modes and constitutive relationship of the specimens under axial tension and splitting tension are further investigated. The results show that the axial tensile strength of RPF RCA concrete first increased and then decreased with the increase in fiber volume content, and was the largest when the fiber volume content was 1.5%, and its strength increased by 21.14% compared with that of recycled concrete. Its lifting rate relative to recycled concrete is between 13.14–21.41%. The change trend of axial tensile strength with the substitution rate of RCA is that it decreases with the increase in substitution rate, and the substitution rate decreases by 9.64% when the substitution rate is 100% compared with 0%. The peak strain first increased and then decreased with the increase in fiber volume content, and the maximum fiber volume content was 1.5%, which increased by 28.19% compared with that of recycled concrete. The peak strain first increased and then decreased with the increase in fiber length-diameter ratio, and the maximum length-diameter ratio was 47.85, which increased by 18.22% compared with that of recycled concrete. The peak strain increased with the increase in the replacement rate of RCA, and the peak strain at 30%, 60% and 100% was 96.22%, 102.45% and 118.09% when the replacement rate was 0%, respectively.



Citation: Wang, J.; Liang, J.; Li, Y.; Hou, W. Tensile Mechanical and Stress-Strain Behavior of Recycling Polypropylene Fiber Recycled Coarse Aggregate Concrete. *Buildings* **2024**, *14*, 1116. <https://doi.org/10.3390/buildings14041116>

Academic Editor: Flavio Stochino

Received: 15 March 2024

Revised: 3 April 2024

Accepted: 11 April 2024

Published: 16 April 2024



Copyright: © 2024 by the authors. Licensee MDPI, Basel, Switzerland. This article is an open access article distributed under the terms and conditions of the Creative Commons Attribution (CC BY) license (<https://creativecommons.org/licenses/by/4.0/>).

1. Introduction

With the acceleration of global urban renewal, nearly 10 billion tons of building rubbish will be produced every year in the world due to the demolition and renovation of old buildings [1]. After classifying, screening, crushing and grinding construction waste, it can be prepared into RCA (with a diameter of 2–3 mm) and used to partially replace natural fine aggregate to prepare RCA Concrete [2,3]. However, during the preparation of RCA, there will be several micro-cracks and initial defects, which will increase the porosity and crushing index of RCA [4,5], thus causing the basic dynamical performances of RCA concrete to generally decline with the comparison of natural coarse aggregate concrete [6,7]. This is also an important reason why it is difficult to popularize recycled concrete for application in engineering. A study by Bárbara Oliveira Paiva and José Maria Franco de Carvalho [8] evaluates the properties of fresh and hardened lightweight concretes, aiming for an optimal mixture design exclusively with lightweight aggregates and mostly plastic waste aggregates. The study shows that, with an optimum dosage, reusing plastic waste in concrete is a viable alternative, contributing to environmental sustainability.

Fiber Recycled Concrete (FRC) is made by mixing discontinuous small randomly distributed fibers in RCA concrete. When fiber is added, the compressive tensile strength [9], creep property, flexural strength [10], tensile strength, toughness [11] and other mechanical properties of fiber recycled concrete will be improved accordingly. It can be seen that adding a certain amount of fiber to RCA concrete is a significant method to enhance the mechanical performance of RCA concrete.

Scholars around the world have drawn important conclusions on the mechanical performances of RCA concrete. Bagherzadeh [12] and Ahmed [13] indicated that when the adjunction of PP fiber with a diameter of 22 μm and length of 19 mm is 0.1–0.3% in RCA concrete, the microscopic structure of RCA concrete can be enhanced and the formation and growth of concrete micro-cracks can be inhibited. In addition, when the RCA concrete is defective, the stress in the concrete can be transferred to the PP fiber due to the bridge connection efficiency of PP fiber, thus enhancing the tensile performance of RCA concrete [14–17]. However, the tensile strength of RCA concrete will be adversely affected by the excessive content of waste PP fiber [16]. Das C S et al. believe that this is due to the high stress generated at the end of the fiber and shorter fibers in the cleavage process, resulting in a decreased RCA concrete tensile strength [17–20]. In addition, the optimal fiber addition rate of RCA concrete will also change with the replacement rate of RCA. Nam J [18] found that adding polyvinyl alcohol and nylon fiber into RCA concrete is helpful to improve the interface bonding ability between cement matrix and RCA, thus improving the dynamical performances of RCA concrete. Thwe Thwe Win [21] found that introducing FM fibers, particularly an FM with a 5 mm diameter and 10 mm length, in the mortar increased both the tensile and flexural strengths. Among the various combinations of FMs studied, a mixture containing 0.15% FMs exhibited the best performance. The findings of this research reveal that FMs can be reused as fibers to enhance the tensile and flexural strengths of cement mortar.

PP packing belts are one of the most widely used packaging strapping materials, but the recycling rate is low and they are usually disposed of in landfills, which causes considerable environmental pollution due to the difficult degradation characteristics. With people paying more and more attention to the environment, new thinking has been carried out on the reuse value of waste, including waste in the form of fiber as a reinforcing material for concrete. This is considered a good waste treatment method to save resources and protect the environment, and has broad development prospects. PP material has the characteristics of non-water absorption [22,23], light weight [24,25] and good acid and alkali resistance [26,27], which makes it possible for it to be used as a concrete reinforcement material. In this regard, a new type of fiber recycled concrete was proposed: recycled PP packing belts were prepared into fibers, and RPF recycled concrete was prepared according to the construction process of fiber reinforced concrete, so as to improve the strength and toughness of recycled concrete. At present, there are few articles that analyze the influence of various parameters of RPF on the mechanical properties of concrete in detail, so this article has research significance. Based on the fact that RPF can enhance the tensile strength, crack resistance and toughness of concrete, this article aims to enhance the tensile performance of concrete by collecting waste materials, such as discarded packing belts in daily life that contain RPF, in order to achieve efficient waste utilization, environmental protection and sustainable development. The RPF used in the experiment was from the non-standard hot melt machine with a transparent packaging belt, with a density of 0.748 g/cm^3 , which is manually cut into the desired shape. Using the RPF recycled by the PP packing belt as the test material, several groups of RPF RCA concrete were designed and fabricated. The length-diameter ratio, volume admixture and RCA substitution rate of RPF were taken as variables. The impact of RPF on the tensile performances of RCA concrete was investigated in depth, which provided a theoretical basis for the recycling of industrial recycled PP packing belts as a strengthening and toughening material of recycled concrete.

2. Experimental Scheme

2.1. Experimental Material

Cement: grade P.O 42.5. Table 1 shows the mineral and chemical component of P.O 42.5 cement.

Table 1. Mineral and chemical component of P.O 42.5 cement.

Mineral Component of P.O 42.5 (%)					
C ₃ S 58.72	C ₂ S 18.54	C ₃ A 6.91	C ₄ AF 9.03	CaSO ₄ 3.16	Other 3.64
Chemical component of P.O 42.5 (%)					
SiO ₂ 21.76	Al ₂ O ₃ 5.15	Fe ₂ O ₃ 2.93	CaO 66.59	MgO 1.21	SO ₃ 2.36

Aggregate: natural gravel and RCA are mixed in a certain proportion as coarse aggregate. The coarse aggregate has a particle size of 5–20 mm. Fine aggregate adopts machine-made sand with fineness modulus of 2.6 and particle size range of 0–4.75 mm. The RCA comes from the abandoned test wall, and its compressive strength is 27.6 MPa, as measured by the rebound meter. After crushing, screening, cleaning and preparation, RCA with a similar size of three axes is selected as far as possible, and needle-shaped aggregate is avoided. Table 2 lists the performance indicators of RCA.

Table 2. Mechanical performance of RCA.

Material	Size (mm)	Performance Density (kg·m ⁻³)	Water Absorption Rate (%)	Crush Index (%)	Stacking Density (kg·m ⁻³)	Mud Content (%)
RCA	5–20	2353	2.68–3.05	12.7	1457	3.55

Fiber: discarded PP fibers with a density of 0.748 g/cm³ are used, which are derived from discarded packing belts in daily life. They are manually cut into the required shape. The mechanical performance indicators can be seen in Table 3.

Table 3. Performance of PP belt.

Material	Peak Load (N)	Peak Strain	Peak Stress (MPa)	Elasticity Modulus (GPa)
RPF	881	0.066	164.59	2.49

RPF size: the size of RPF is measured by digital vernier caliper and steel tape measure with an accuracy of 0.01 mm. The average width is 1.72 mm, the thickness is between 0.45–0.55 mm, the average value is 0.5 mm, the equivalent diameter of the cross-section is 1.046 mm, and the average length of each group of fibers is 30.02 mm, 39.77 mm, 50.07 mm and 58.94 mm, respectively. The length-diameter ratios are 28.69, 38.01 and 47.

2.2. Proportioning of RCA Concrete

The proportioning of RCA concrete was designed according to the Chinese standard JGJ/T443 [28] and 55-2011 [29]. The incorporation of RPF will produce a large number of fiber mortar clumps during mixing, and the fluidity will decrease, resulting in uneven distribution of concrete fiber and aggregate [30–32]. Therefore, in the process of material configuration, cement, sand, RCA and RPF are dry mixed, and water is added in two batches for secondary mixing after mixing evenly.

As there are many initial imperfections in the RCA, it will absorb water, resulting in a decrease in hydration water content and the water-binder ratio of RCA concrete [33].

To reduce the RCA water absorption to prevent RPF RCA concrete water cement ratio changes [34–36], the mixing water of recycled concrete is hydration water and additional water; the additional water is determined by the water absorption rate. The number and mix ratio of all specimens in this project can be seen in Table 4.

Table 4. Proportion of group.

Group	Proportioning of RCA Concrete (kg/m ³)							
	Cement	Sand	Water	RCA	Crushed Stones	RPF	Additional Water	Slump (mm)
RC-100-0	590	704.48	295	810.53	0	0	23.26	48
FRC-100-5-50	590	704.48	295	810.53	0	3.74	23.26	47
FRC-100-10-50	590	704.48	295	810.53	0	7.48	23.26	45
FRC-100-15-50	590	704.48	295	810.53	0	11.22	23.26	44
FRC-100-20-50	590	704.48	295	810.53	0	14.96	23.26	43
FRC-100-15-30	590	704.48	295	810.53	0	11.22	23.26	44
FRC-100-15-40	590	704.48	295	810.53	0	11.22	23.26	44
FRC-100-15-60	590	704.48	295	810.53	0	11.22	23.26	44
FRC-60-15-50	590	704.48	295	486.32	324.21	11.22	13.96	46
FRC-30-15-50	590	704.48	295	243.16	567.37	11.22	6.98	47
FNC-0-15-50	590	704.48	295	0	810.53	11.22	0	48

RC: Recycled Concrete, FRC: Fiber Recycled Concrete, FNC: Fiber Reinforced Concrete.

2.3. Specimen Preparation

A total of 11 experimental groups are shown in Table 4. There are six specimens in each group and each group has three test blocks for cleavage tensile strength, stress-strain curve and axial tensile strength test. Specimen size of 150 × 150 × 150 mm is for cleavage tensile strength specimen and 150 × 100 × 460 mm is for axial tensile strength of the fusiform specimen. In addition, the tensile elastic modulus, axial tensile peak and ultimate strain of RPF RCA concrete can be measured synchronously in the axial tensile $\sigma - \epsilon$ test.

To ensure the same environmental temperature and other factors during the production of specimens, the same batch of concrete specimens was completed at the same time in accordance with standard curing requirements, at constant temperature and humidity for 28 days.

2.4. Test Methods

2.4.1. Cleavage Tensile Strength Test

The experimental methods refer to GB/T50080 [37], GB/T50081-2019 [38], BS EN 12350 [39] and BS EN 12390 [40–43]. After curing the test block for 28 d, check that the dimension deviation of the test block does not exceed 1 mm. The test block is installed on the cleavage tensile test fixture. The pad, pad strip and specimen are placed on the loading platform of 60 t universal testing machine. The test apparatus and data collection and analysis system are arranged as can be seen in Figure 1. First, start the loading machine at the loading rate of 0.2 mm/min. When the testing machine pressure increase is slowed down, keep the loading machine at a constant rate until the specimen is thoroughly destroyed.



Figure 1. The device used for loading.

2.4.2. Axial Tensile Strength Test

After the test block reaches the curing stage, install and place the test block and the test device on the 60 t universal test machine and set the test parameters. Start the testing machine and load it to 0.5 MPa. Check whether the strain difference on the 4 screws is less than 10%. If so, adjust the strain value of each screw through the knob nut until the strain difference between the 4 screws is less than 10%. Before the failure of the specimen, the loading has been carried out at the displacement rate of 0.04 mm/min. The test steel frame is composed of 48.9-level M20 screws and 2 25 mm thick high-strength steel plates, as shown in Figure 2.



Figure 2. Test setups.

3. Results and Discussion

3.1. Cleavage Tensile Strength

Through Figure 3, it is shown that the cleavage tensile failure mode of RPF RCA concrete is different from that of non-fiber recycled concrete. Its failure cracks are not completely perpendicular to the bearing surface and are more irregular, and the concrete on the failure surface is less spalling. By checking the cross-section, it can be found that the fiber failure in concrete is both fiber tensile fracture and fiber bonding failure.



Figure 3. Failure mode. (a) Failure mode of split tensile; (b) Section of splitting tensile.

The cleavage tensile experimental results of specimens in each group are listed in Table 5. A conclusion can be drawn that the cleavage tensile performances of RCA concrete have made a big difference due to the incorporation of RPF.

Table 5. Each performance index of each test block.

Group	Cleavage Tensile Strength		Axial Tensile		
	(MPa)	Peak Strength (MPa)	Initial Crack Strength (MPa)	Initial Crack Strain ($\mu\epsilon$)	Peak Strain ($\mu\epsilon$)
RC-100-0	2.46	2.14	1.14	87.65	152.98
FRC-100-5-50	2.55	2.15	1.17	91.15	158.97
FRC-100-10-50	2.69	2.34	1.22	96.10	178.93
FRC-100-15-50	2.98	2.53	1.30	107.65	196.10
FRC-100-20-50	2.61	2.26	1.17	94.88	166.52
FRC-100-15-30	2.87	2.49	1.34	109.02	178.85
FRC-100-15-40	2.91	2.49	1.31	108.87	178.20
FRC-100-15-60	2.79	2.43	1.25	101.11	182.22
FRC-60-15-50	2.99	2.56	1.35	108.65	170.12
FRC-30-15-50	3.11	2.62	1.42	109.52	166.78
FNC-0-15-50	3.23	2.80	1.50	111.86	166.05

The Influence of RCA Replacement Rate

Figure 4c shows that, with the rise in the replacement ratio of RCA, the cleavage tensile strength of RPF RCA concrete gradually goes down. This is because there are several initial cracks in the RCA concrete. Due to the rise in RCA replacement rate in concrete, the initial cracks in concrete also increase, thus producing a negative effect on RPF RCA concrete strength. From the standard deviation distribution in the three figures, it can be seen that the standard deviation value is the largest under the aspect ratio condition, and the standard deviation value is close to that under the fiber volume parameter and aggregate substitution rate condition.

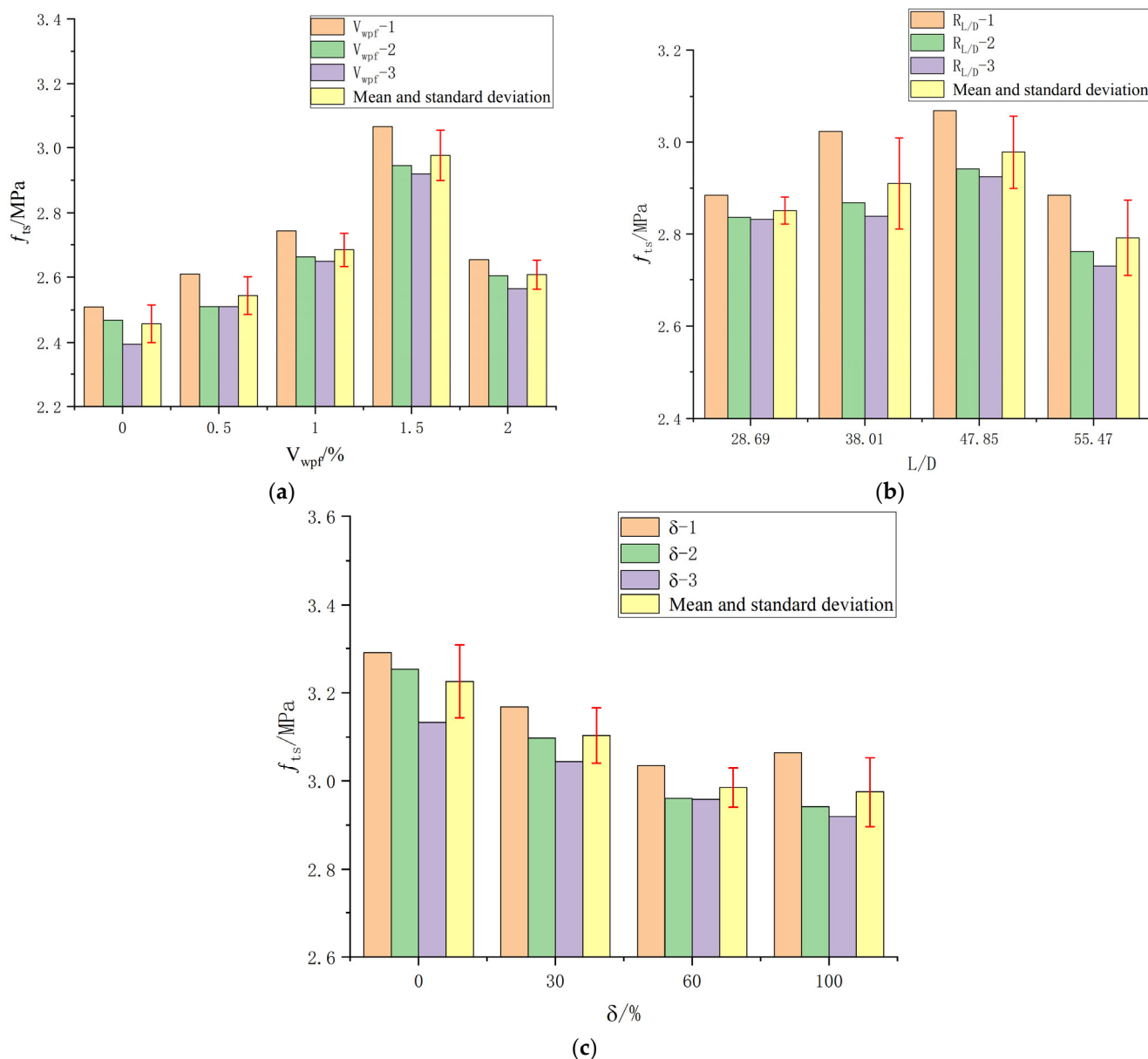


Figure 4. Influence curves of various parameters on cleavage tensile strength. (a) Influence curve of fiber volume content group; (b) Influence curve of fiber length-diameter ratio group; (c) Influence curve of replacement rate of an RCA group.

3.2. Axial Tensile Test Strength

Figure 5 shows the tensile failure form of recycled concrete tends to be irregular following the addition of RPF. The section is basically the minimum section, but the development direction is irregular, and there are several secondary cracks near the main section; the failure shows certain plastic characteristics.



Figure 5. Failure mode of axial tensile test.

As indicated in Table 3, the incorporation of RPF improves the axial tensile strength of RCA concrete.

Figure 6 shows the incidence of various impact parameters on the initial-crack (I-C) strength and axial tensile strength of RPF RCA concrete. Figure 6a indicates the impact of the fiber volume addition ratio on the axial tensile strength and I-C strength. It can be found that the axial tensile strength and I-C strength increase first with the rise in the fiber volume addition ratio. When the fiber volume addition ratio reaches 1.5%, the axial tensile strength and I-C strength of concrete reach the maximum. Subsequently, when the fiber volume addition ratio exceeds 1.5%, the axial tensile strength and initial crack strength decrease with the rise in the RPF volume addition ratio. The influence principle of fiber volume addition ratio on axial tensile strength is the same as that of cleavage tensile.

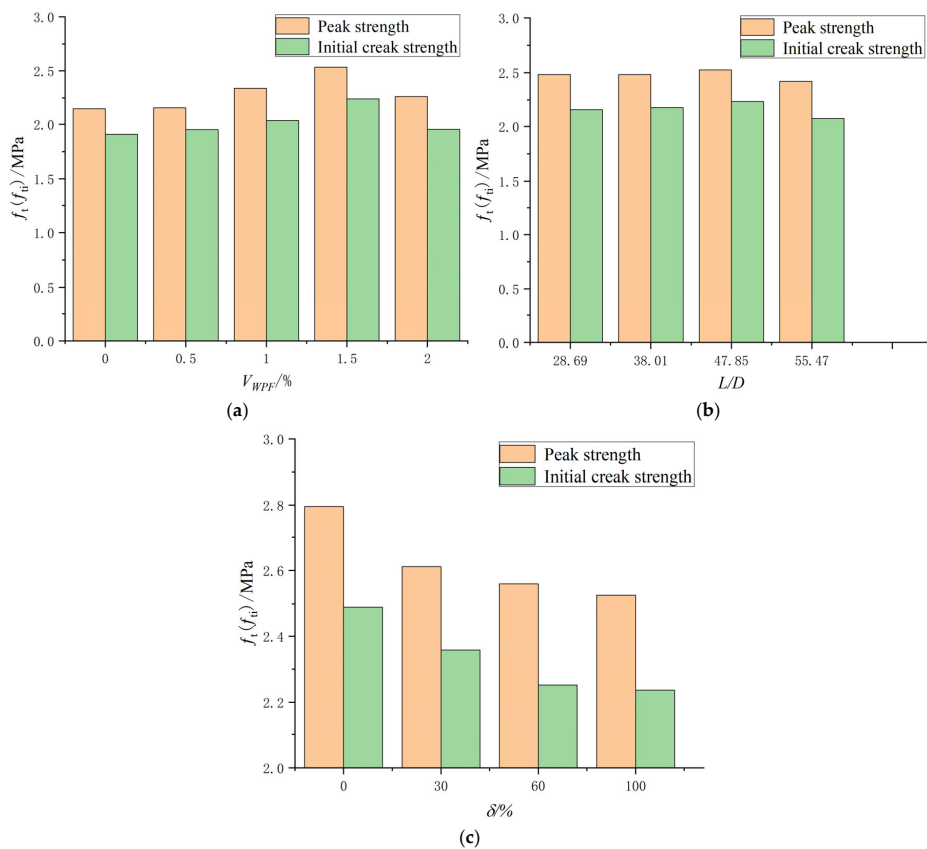


Figure 6. Initial crack strength and peak strength of RPF RCA concrete. (a) Influence curve of fiber volume content; (b) Influence curve of fiber length-diameter ratio; (c) Influence curve of replacement rate of RCA.

It can be found from Figure 6b, the axial tensile strength and initial crack strength of RPF RCA concrete increase at first and then drop with the rise in the fiber length-diameter ratio. When the aspect ratio of RPF reaches 47.85, the axial tensile strength and initial crack strength reach the peak.

It can be shown through Figure 6c that, with the increase in RCA replacement ratio, both the axial tensile strength and initial cracking strength are decreased.

3.3. Axial Tensile Initial Crack Strain and Peak Strain

The impact of RPF volume additional ratio on the initial crack (I-C) strain and peak strain of RPF concrete can be seen in Figure 7a. The conclusion can be drawn that both I-C strain and peak tensile strain increased first and decreased later, due to the increase in the RPF volume additional ratio.

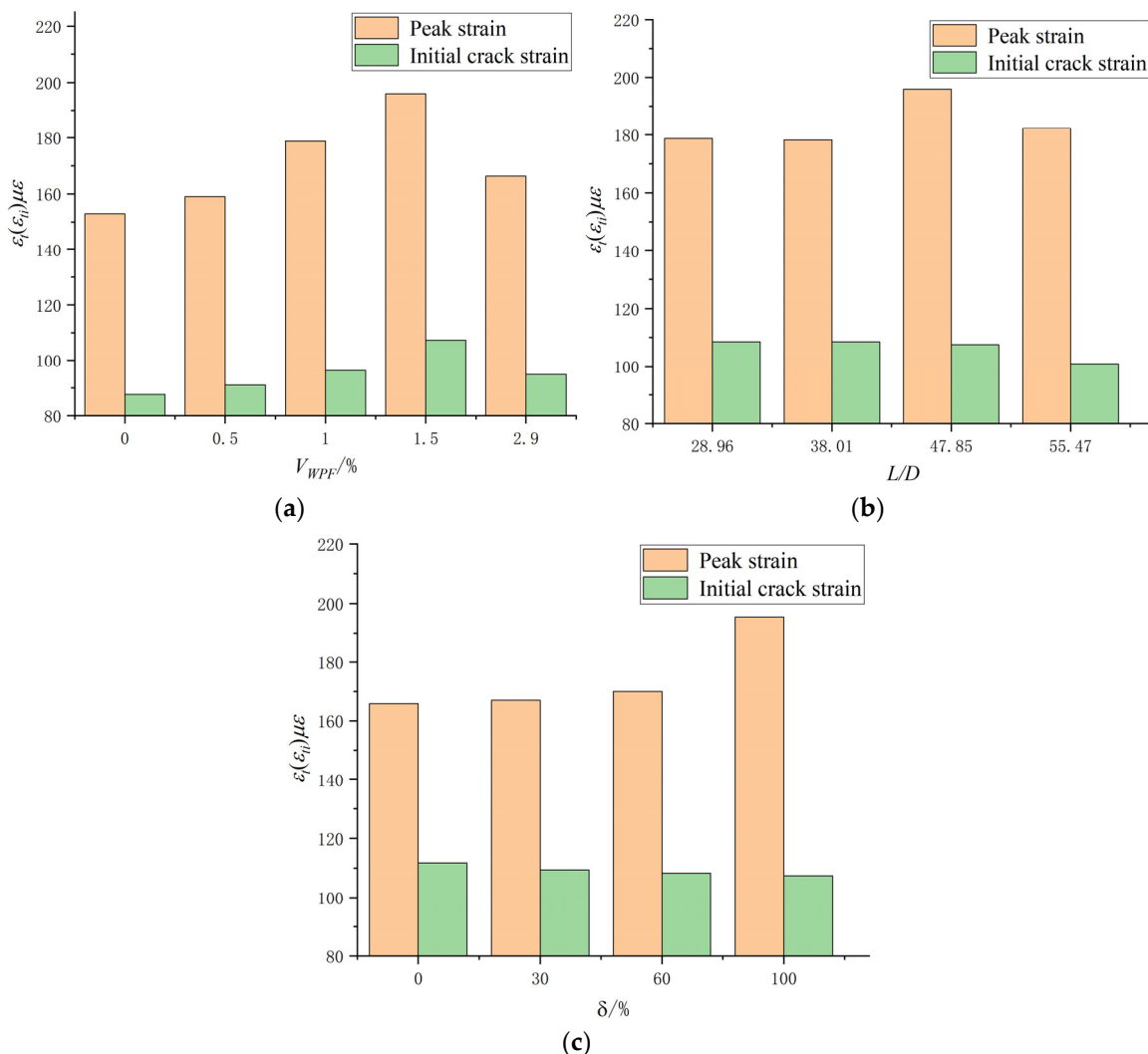


Figure 7. Peak strain and initial cracking strain of RPF RCA concrete. (a) Influence curve of fiber volume content; (b) Influence curve of fiber length-diameter ratio; (c) Deformation influence curve of replacement rate of RCA.

Figure 7b analyzes the influence of the RPF length-diameter (L-D) ratio on the initial crack strain and peak strain of RPF RCA concrete. Through Figure 7b, the fiber aspect ratio has a slight effect on the I-C strain, and the overall initial crack strain decreases with the increase in the L-D ratio. Due to the increase in the L-D ratio, the peak strain of RCA concrete increases at first and then decreases last.

Figure 7c shows the influence of the replacement ratio of RCA on the deformation. It can be found that the incipient strain goes down with the increase in the replacement rate, while the peak strain raises with the rise in the replacement rate of RCA.

3.4. Analysis of the Stress-Strain Relationship

As shown in Figure 8, the impacts of RCA and RPF on the $\sigma - \varepsilon$ behavior of concrete are significant. The $\sigma - \varepsilon$ curve of RPF RCA concrete is similar to that of FNC. Compared with FNC, RCA reduces the peak strength of RCA concrete. It is precisely because the addition of RPF can not only enhance the axial tensile strength of RCA concrete, but also increase the peak tensile strain of RCA concrete. The influence of different factors on the axial tensile $\sigma - \varepsilon$ behavior of FRC can be seen in Figure 9.

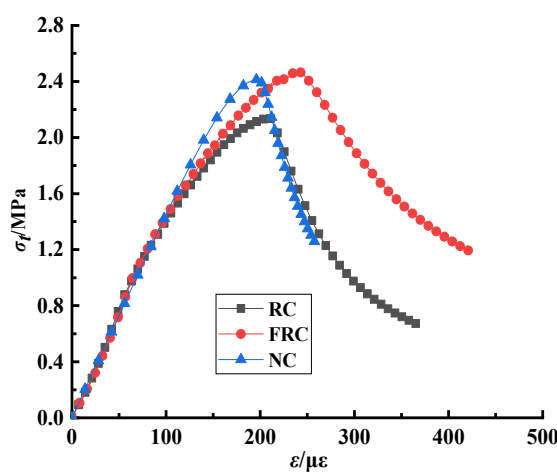


Figure 8. The axial tensile stress-strain behavior of concrete.

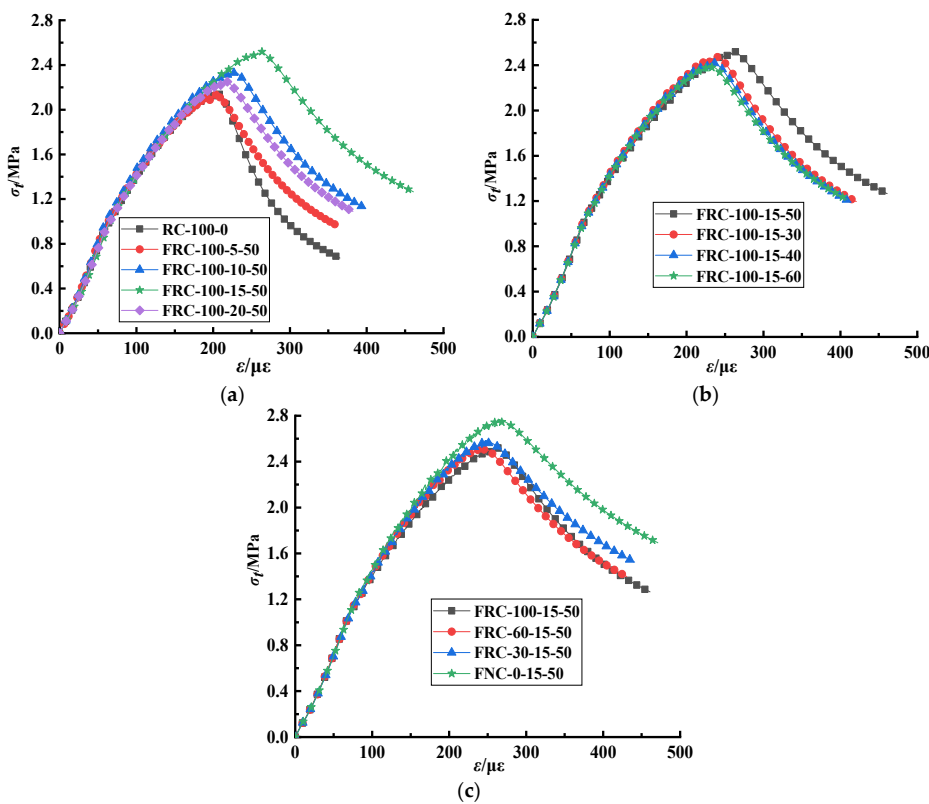


Figure 9. The axial tensile stress-strain behavior of FRC. (a) Influence of fiber volume; (b) Influence of fiber length-diameter ratio; (c) Influence of replacement rate of RCA.

3.5. Stress-Strain Constitutive Models

In order to deeply and comprehensively understand the tensile properties of RCA concrete materials, it is necessary to study the tensile stress-strain relationship.

3.5.1. Axial Tensile Stress-Strain Constitutive Model of NC

Recently, researchers have proposed many NC axial tensile stress-strain constitutive models. Among them, the segmented model was proposed by Guo Zhenhai [44,45] in 1993. Due to its simple form and clear meaning, it has been broadly used in the world. The mathematical equation of the $\sigma - \varepsilon$ model is as follows in Equation (1):

$$\sigma/f_t = \begin{cases} 1.2(\varepsilon/\varepsilon_p) - 0.2(\varepsilon/\varepsilon_p)^6 & (\varepsilon/\varepsilon_p) \leq 1 \\ \frac{(\varepsilon/\varepsilon_p)}{\alpha_t[(\varepsilon/\varepsilon_p)-1]^{1.7} + (\varepsilon/\varepsilon_p)} & (\varepsilon/\varepsilon_p) > 1 \end{cases} \quad (1)$$

$$\alpha_t = 0.312f_t^2 \quad (2)$$

The CDP model is a widely used concrete constitutive model in the world [46]. It has become an important reference for concrete structure design [47]. The mathematical expression of the constitutive model is as follows (3):

$$\sigma = (1 - d_t)E_c\varepsilon \quad (3)$$

$$d_t = \begin{cases} 1 - \rho_t[1.2 - 0.2x^5] & x \leq 1 \\ 1 - \frac{\rho_t}{\alpha_t(x-1)^{1.7} + x} & x > 1 \end{cases} \quad (4)$$

$$x = \varepsilon/\varepsilon_{t,r} \quad (5)$$

$$\rho_t = f_{t,r}/E_c\varepsilon_{t,r} \quad (6)$$

3.5.2. Axial Tensile Stress-Strain Constitutive Model of FRC

Equation (1) is simple in form and has good accuracy in fitting the $\sigma - \varepsilon$ curve of axial tensile performances. In this paper, this equation is used to fit the full curve of the axial tensile $\sigma - \varepsilon$ of RPF RCA concrete.

$$\sigma/f_t = \begin{cases} a(\varepsilon/\varepsilon_p) + (1.5 - 1.25a)(\varepsilon/\varepsilon_p)^2 + (0.25a - 0.5)(\varepsilon/\varepsilon_p)^6 & (\varepsilon/\varepsilon_p) \leq 1 \\ \frac{(\varepsilon/\varepsilon_p)}{\alpha_t[(\varepsilon/\varepsilon_p)-1]^{1.45} + (\varepsilon/\varepsilon_p)} & (\varepsilon/\varepsilon_p) > 1 \end{cases} \quad (7)$$

Equation (7) is used to fit the measured $\sigma - \varepsilon$ curve, and the fitted curve is shown in Figure 10. The fitted parameter values are shown in Table 6.

Table 6. Tensile constitutive parameters.

Group	Parameters	
	a	α_t
RC-100-0	1.742	5.883
FRC-100-5-50	1.788	3.214
FRC-100-10-50	1.780	2.947
FRC-100-15-50	1.733	2.645
FRC-100-20-50	1.670	2.844
FRC-100-15-30	1.681	2.876
FRC-100-15-40	1.646	2.731
FRC-100-15-60	1.693	2.597
FRC-60-15-50	1.691	2.140
FRC-30-15-50	1.760	1.844
FNC-0-15-50	1.714	1.682

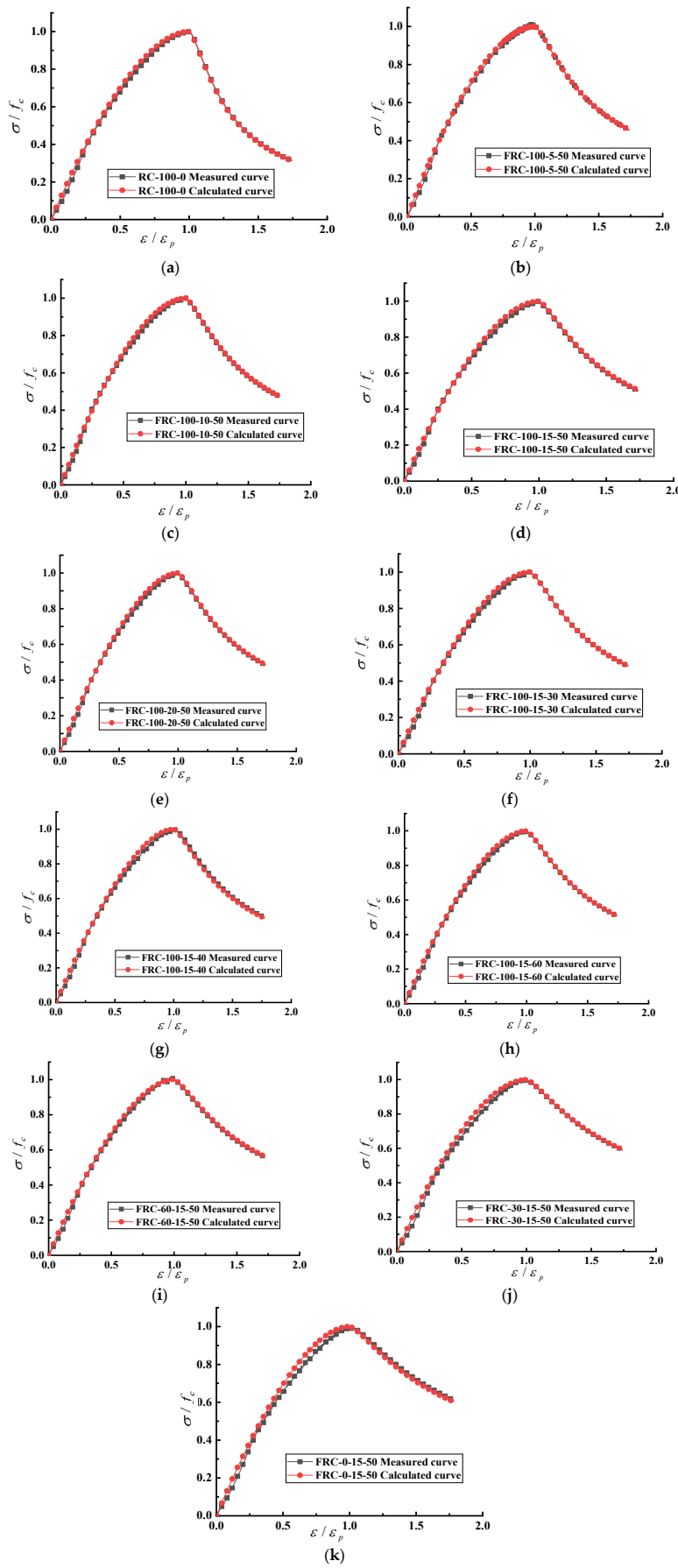


Figure 10. Tensile stress-strain fitting curve. (a) RC-100-0 tensile stress-strain fitting curve; (b) FRC-100-5-50

tensile stress-strain fitting curve; (c) FRC-100-10-50 tensile stress-strain fitting curve; (d) FRC-100-15-50 tensile stress-strain fitting curve; (e) FRC-100-20-50 tensile stress-strain fitting curve; (f) FRC-100-15-30 tensile stress-strain fitting curve; (g) FRC-100-15-40 tensile stress-strain fitting curve; (h) FRC-100-15-60 tensile stress-strain fitting curve; (i) FRC-60-15-50 tensile stress-strain fitting curve; (j) FRC-30-15-50 tensile stress-strain fitting curve; (k) FNC-0-15-50 tensile stress-strain fitting curve.

3.6. Tensile Toughness

The equivalent tensile toughness index of RPF recycled concrete can be calculated by the formula (8), as shown in Table 7 and Figure 11.

$$W_{tu} = f_{te} \times \frac{\delta}{l} = \frac{\Omega_u}{A\delta_u} \times \frac{\delta_u}{l} = \frac{\Omega_u}{Al} \quad (8)$$

Table 7. Equivalent tensile toughness index.

Group	$W_{tu}^{1,0}$ (Pa)	Gain Ratio
RC-100-0	207.6905	100.00%
FRC-100-5-50	217.9078	104.92%
FRC-100-10-50	266.6963	128.41%
FRC-100-15-50	309.6578	149.10%
FRC-100-20-50	234.8848	113.09%
FRC-100-15-30	234.8848	113.09%
FRC-100-15-40	274.8961	132.36%
FRC-100-15-60	276.7001	133.23%
FRC-60-15-50	272.0142	130.97%
FRC-30-15-50	276.1605	132.97%
FNC-0-15-50	291.8175	140.51%

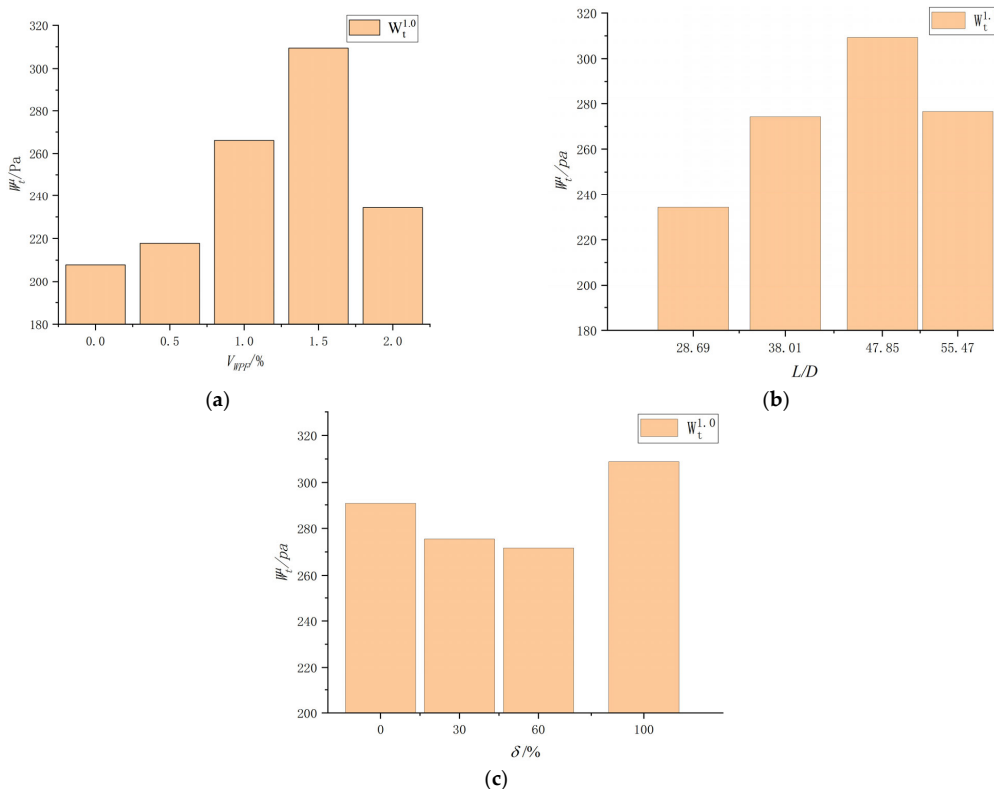


Figure 11. Equivalent tensile toughness index curve. (a) Influence of fiber volume; (b) Influence of fiber length-diameter ratio; (c) Influence of replacement rate of RCA.

4. Conclusions

In this chapter, the axial tensile strength, tensile stress-strain curve and peak tensile strain under different fiber volume content, fiber length-diameter ratio and RCA substitution rate are obtained, using 11 groups of RPF recycled concrete axial tensile test blocks, and the following conclusions are obtained:

- (1) The axial tensile strength first increased and then decreased with the increase in fiber volume content, and was largest when the fiber volume content was 1.5%. Its strength increased by 18.22% compared with recycled concrete, and the change trend of axial tensile strength with fiber length-diameter ratio was roughly increased first and then decreased with the increase in length-diameter ratio, but the change range was not large, and its lifting rate relative to recycled concrete was between 5.61–18.22%. The change trend of axial tensile strength with the substitution rate of RCA is that it decreases with the increase in substitution rate, and the substitution rate decreases by 9.64% when the substitution rate is 100% compared with 0%.
- (2) The peak strain first increased and then decreased with the increase in fiber volume content, and the fiber volume content was largest when the fiber volume content was 1.5%, which was 28.19% higher than that of recycled concrete. The peak strain increased first and then decreased with the increase in the fiber length-diameter ratio, and the maximum was 47.85. The peak strain increased with the increase in the substitution rate of RCA, and the peak strain at 30%, 60% and 100% was 100.44%, 102.45% and 118.09% at 0%, respectively.
- (3) The equivalent tensile toughness index $W_{tu}^{1.0}$ of RPF recycled concrete first increased and then decreased with the increase in fiber volume content, and the volume content was the best when the volume content was 1.5%. With the increase in the fiber aspect ratio, the tensile toughness index $W_{tu}^{1.0}$ first decreased and then increased, and the substitution of natural aggregate by RCA may enhance the energy dissipation capacity of RPF recycled concrete.
- (4) The constitutive model of the tensile rising section of the RPF recycled concrete is proposed, which is consistent with the actual rising section of the stress-strain curve.

Author Contributions: Conceptualization, J.L.; Methodology, J.L. and Y.L.; Software, J.L.; Validation, J.L.; Formal analysis, J.L., Y.L. and W.H.; Investigation, Y.L.; Resources, Y.L. and W.H.; Data curation, Y.L.; Writing – original draft, J.W.; Writing – review & editing, J.W.; Visualization, J.W.; Supervision, J.W.; Project administration, J.W. and W.H.; Funding acquisition, W.H. All authors have read and agreed to the published version of the manuscript.

Funding: This research received no external funding.

Data Availability Statement: The data presented in this study are available in the article.

Conflicts of Interest: The authors declare no conflict of interest.

Notation

ε	Concrete tensile strain
σ	Concrete tensile stress
f_t	Peak tensile stress in concrete
ε_p	Peak tensile strain of concrete
d_t	evolution parameter of concrete uniaxial tensile damage
α_t	Parameter values for the falling section of the uniaxially tensile stressed concrete strain curve
$\varepsilon_{t,r}$	Peak tensile strains in concrete corresponding to representative values of uniaxial tensile strength $f_{t,r}$
W_{tu}	Equivalent tensile toughness index of concrete (Pa)
l	Vertical deformation scale of axial tensile test block (mm)
f_{te}	Equivalent tensile strength of concrete (MPa)
Ω_u	The area under the load-deformation curve when the vertical deformation is δ_u (N·mm)
δ_u	The longitudinal deformation when the load is reduced to a multiple of the ultimate load u (mm)
A	Pressure area of axial compression test block (mm^2)

References

1. Mejia-Ballesteros, J.E.; Rodier, L.; Filomeno, R.; Savastano, H., Jr.; Fiorelli, J.; Rojas, M.F. Influence of the fiber treatment and matrix modification on the durability of eucalyptus fiber reinforced composites. *Cem. Concr. Compos.* **2021**, *124*, 104280. [[CrossRef](#)]
2. Ferriz-Papi, J.A.; Weekes, E.; Whitehead, N.; Lee, A. A cost-effective recycled aggregates classification procedure for construction and demolition waste evaluation. *Constr. Build. Mater.* **2022**, *324*, 126642. [[CrossRef](#)]
3. Frazão, C.; Díaz, B.; Barros, J.; Bogas, J.A.; Toptan, F. An experimental study on the corrosion susceptibility of Recycled Steel Fiber Reinforced Concrete. *Cem. Concr. Compos.* **2019**, *96*, 138–153. [[CrossRef](#)]
4. Tran, D.L.; Mouret, M.; Cassagnabère, F.; Phung, Q.T. Effects of intrinsic granular porosity and mineral admixtures on durability and transport properties of recycled aggregate concretes. *Mater. Today Commun.* **2022**, *33*, 104709. [[CrossRef](#)]
5. Wu, H.; Wang, C.; Ma, Z. Drying shrinkage, mechanical and transport properties of sustainable mortar with both recycled aggregate and powder from concrete waste. *J. Build. Eng.* **2022**, *49*, 104048. [[CrossRef](#)]
6. Yang, Z.C.; Han, L.H.; Hou, C. Performance of recycled aggregate-filled steel tubular columns under combined compression and shear load. *Eng. Struct.* **2022**, *253*, 113771. [[CrossRef](#)]
7. El-Hawary, M.; Al-Sulily, A. Internal curing of recycled aggregates concrete. *J. Clean. Prod.* **2020**, *275*, 122911. [[CrossRef](#)]
8. Resende, D.M.; de Carvalho, J.M.F.; Paiva, B.O.; Gonçalves, G.d.R.; Costa, L.C.B.; Peixoto, R.A.F. Sustainable Structural Lightweight Concrete with Recycled Polyethylene Terephthalate Waste Aggregate. *Buildings* **2024**, *14*, 609. [[CrossRef](#)]
9. Wang, J.; Li, Y.; Qiu, Z.; Zhang, Y. Experimental research on compressive properties of recycling polypropylene (PP) fiber recycled coarse aggregate concrete. *J. Build. Eng.* **2023**, *76*, 107403. [[CrossRef](#)]
10. Li, Z.; Shen, A.; Zeng, G.; Chen, Z.; Guo, Y. Research progress on properties of basalt fiber-reinforced cement concrete. *Mater. Today Commun.* **2022**, *33*, 104824. [[CrossRef](#)]
11. Aslani, F.; Hou, L.; Nejadi, S.; Sun, J.; Abbasi, S. Experimental analysis of fiber-reinforced recycled aggregate self-compacting concrete using waste recycled concrete aggregates, polypropylene, and steel fibers. *Struct. Concr.* **2019**, *20*, 1670–1683. [[CrossRef](#)]
12. Bagherzadeh, R.; Sadeghi, A.H.; Latifi, M. Utilizing polypropylene fibers to improve physical and mechanical properties of concrete. *Text. Res. J.* **2012**, *82*, 88–96. [[CrossRef](#)]
13. Kazmi, S.M.S.; Munir, M.J.; Wu, Y.F.; Patnaikuni, I.; Zhou, Y.; Xing, F. Axial stress-strain behavior of macro-synthetic fiber reinforced recycled aggregate concrete. *Cem. Concr. Compos.* **2019**, *97*, 341–356. [[CrossRef](#)]
14. Hanumesh, B.M.; Harish, B.A.; Venkata Ramana, N. Influence of polypropylene fibers on recycled aggregate concrete. *Mater. Today Proc.* **2018**, *5*, 1147–1155. [[CrossRef](#)]
15. Hunashikatti, G.M.; Pradhan, S.; Bara, S.V. Partially hydrated recycled aggregate concrete: A systematic approach towards sustainable development. *Constr. Build. Mater.* **2018**, *186*, 537–549. [[CrossRef](#)]
16. Ye, P.; Chen, Z.; Su, W. Mechanical properties of fully recycled coarse aggregate concrete with polypropylene fiber. *Case Stud. Constr. Mater.* **2022**, *17*, e01352. [[CrossRef](#)]
17. Das, S.; Sinah, P.; Negi, V.S. Strength and durability properties of polypropylene fiber reinforced recycled coarse aggregate concrete. *Indian Concr. J.* **2018**, *94*, 62–69.
18. Nam, J.; Kim, G.; Yoo, J.; Choe, G.; Kim, H.; Choi, H.; Kim, Y. Effectiveness of fiber reinforcement on the mechanical properties and shrinkage cracking of recycled fine aggregate concrete. *Materials* **2016**, *9*, 131. [[CrossRef](#)] [[PubMed](#)]
19. Mudadu, A.; Tiberti, G.; Germano, F.; Plizzari, G.A.; Morbi, A. The effect of fiber orientation on the post-cracking behavior of steel fiber reinforced concrete under bending and uniaxial tensile tests. *Cem. Concr. Compos.* **2018**, *93*, 274–288. [[CrossRef](#)]
20. Xiao, J.; Poon, C.S.; Zhao, Y.; Wang, Y.; Ye, T.; Duan, Z.; Peng, L. Fundamental behavior of recycled aggregate concrete—Overview II: Durability and enhancement. *Mag. Concr. Res.* **2022**, *74*, 1011–1026. [[CrossRef](#)]
21. Win, T.T.; Jongvivatsakul, P.; Jirawattanasomkul, T.; Prasittisopin, L.; Likitlersuang, S. Use of polypropylene fibers extracted from recycled surgical face masks in cement mortar. *Constr. Build. Mater.* **2023**, *391*, 131845. [[CrossRef](#)]
22. Al-Quraishi, H.; Abdulkhudhur, R.; Abdulazeez, A. Shear Strength Behavior of Fiber Reinforced Recycled Aggregate Concrete Beams. *Int. Rev. Civ. Eng.* **2021**, *12*, 4183. [[CrossRef](#)]
23. McGinnis, M.J.; Davis, M.; de la Rosa, A.; Weldon, B.D.; Kurama, Y.C. Quantified sustainability of recycled concrete aggregates. *Mag. Concr. Res.* **2017**, *69*, 1203–1211. [[CrossRef](#)]
24. Carneiro, J.A.; Lima, P.R.L.; Leite, M.B.; Toledo Filho, R.D. Compressive stress-strain behavior of steel fiber reinforced-recycled aggregate concrete. *Cem. Concr. Compos.* **2014**, *46*, 65–72. [[CrossRef](#)]
25. Dinh, N.H.; Park, S.H.; Choi, K.K. Effect of dispersed micro-fibers on tensile behavior of uncoated carbon textile-reinforced cementitious mortar after high-temperature exposure. *Cem. Concr. Compos.* **2021**, *118*, 103949. [[CrossRef](#)]
26. Feng, Z.; Shen, D.; Luo, Y.; Huang, Q.; Liu, Z.; Jiang, G. Effect of polypropylene fiber on early-age properties and stress relaxation of ultra-high-performance concrete under different degrees of restraint. *J. Build. Eng.* **2023**, *68*, 106035. [[CrossRef](#)]
27. Vijayan, V.; Jayakesh, K.; Anand, K.B. Mechanical properties of recycled aggregates concrete with sisal fiber and silica fume. *Mater. Today Proc.* **2022**, *65*, 1887–1894. [[CrossRef](#)]
28. JGJ/T 443-2018; Technical Standard for Recycled Concrete Structure. Ministry of Housing and Urban Rural Development of the People's Republic of China: Beijing, China, 2018.
29. JGJ 55-2011; Specification for Mix Proportion Design of Ordinary Concrete. Ministry of Housing and Urban Rural Development of the People's Republic of China: Beijing, China, 2011.

30. Magdalena, P.M.; Kaszynska, M. Mechanical performance and environmental assessment of sustainable concrete reinforced with recycled end-of-life tyre fibers. *Materials* **2021**, *14*, 1–20.
31. Ahmadi, M.; Farzin, S.; Hassani, A.; Motamed, M. Mechanical properties of the concrete containing recycled fibers and aggregates. *Constr. Build. Mater.* **2017**, *144*, 392–398. [[CrossRef](#)]
32. Bui, N.K.; Satomia, T.; Takahashia, H. Recycling woven plastic sack waste and PET bottle waste as fiber in recycled aggregate concrete: An experimental study. *Waste Manag.* **2018**, *78*, 79–93. [[CrossRef](#)]
33. Ferrara, G.; Pepe, M.; Martinelli, E.; Tolêdo Filho, R.D. Tensile behavior of flax textile reinforced lime-mortar: Influence of reinforcement amount and textile impregnation. *Cem. Concr. Compos.* **2021**, *119*, 103984. [[CrossRef](#)]
34. Katkhuda, H.; Shatarat, N. Improving the mechanical properties of recycled concrete aggregate using chopped basalt fibers and acid treatment. *Constr. Build. Mater.* **2017**, *140*, 328–335. [[CrossRef](#)]
35. Tam, V.W.; Wattage, H.; Le, K.N.; Butera, A.; Soomro, M. Hybrid methods to improve microstructure of recycled concrete and brick aggregate for high-grade concrete production. *Mag. Concr. Res.* **2022**, *75*, 17–31. [[CrossRef](#)]
36. Li, L.; Ruan, S.; Zeng, L. Mechanical properties and constitutive equations of concrete containing a low volume of tire rubber particles. *Constr. Build. Mater.* **2014**, *70*, 291–308. [[CrossRef](#)]
37. GB/T 50080-2016; Standard for Test Method of Performance on Ordinary Fresh Concrete. Ministry of Housing and Urban Rural Development of the People's Republic of China: Beijing, China, 2016.
38. GB/T 50081-2019; Standard for Test Method of Mechanical Properties on Ordinary Concrete. Ministry of Housing and Urban Rural Development of the People's Republic of China: Beijing, China, 2019.
39. BS EN 12350-2-2009; Testing Fresh Concrete-Slump-Test. Comité Européen de Normalisation: Brussels, Belgium, 2009.
40. BS EN 12390-3-2009; Testing Hardened Concrete-Compressive Strength of Test Specimens. Comité Européen de Normalisation: Brussels, Belgium, 2009.
41. BS EN 12390-5-2009; Testing Hardened Concrete-Flexural Strength of Test Specimens. Comité Européen de Normalisation: Brussels, Belgium, 2009.
42. BS EN 12390-6-2009; Testing Hardened Concrete-Tensile Cleavage Strength of Test Specimens. Comité Européen de Normalisation: Brussels, Belgium, 2009.
43. BS EN 12390-13-2013; Testing Hardened Concrete-Determination of Secant Modulus of Elasticity in Compression. Comité Européen de Normalisation: Brussels, Belgium, 2013.
44. Guo, Z.; Zhang, X.; Zhang, D. Experimental study on the stress-strain curve of concrete. *J. Build. Struct.* **1982**, 1–12.
45. Guo, Z.; Nan, J.; Shi, X. Temperature stress coupled constitutive relationship of concrete. *J. Tsinghua Univ. (Nat. Sci. Ed.)* **1997**, 89–92. [[CrossRef](#)]
46. Han, R.; Zhao, S.; Qu, F. Experimental study on the tensile performance of steel fiber reinforced concrete. *J. Civ. Eng.* **2006**, 63–67.
47. Yang, M.; Huang, C. Experimental study on the axial tensile performance of steel fiber high-strength concrete. *J. Civ. Eng.* **2006**, 55–61.

Disclaimer/Publisher’s Note: The statements, opinions and data contained in all publications are solely those of the individual author(s) and contributor(s) and not of MDPI and/or the editor(s). MDPI and/or the editor(s) disclaim responsibility for any injury to people or property resulting from any ideas, methods, instructions or products referred to in the content.